COMPARISON OF MONOTONIC AND CYCLIC PROPERTIES OF DUCTILE IRONS IN THE AFS/DOE STRAIN-LIFE FATIGUE DATABASE FOR CAST IRON

J. Tartaglia
Element Materials Technology, Wixom, MI, USA

Abstract

A strain-life fatigue database for cast irons was developed utilizing American Foundry Society (AFS) and the United States Department of Energy (DOE) funding. The database contains monotonic and cyclic property data, as well as the associated chemical analysis and microstructural data for a variety of cast irons, including gray, ductile, compacted graphite, and white cast irons.

This paper first reviews the contents and format of the database. The database and its associated report contain no comparative analysis of any of the cast iron grades. The fresh approach of this paper is to analyze and compare the data across each section size and strength-ductility combination for four ductile iron grades, i.e., ferritic 60-40-18, ferritic-pearlitic 65-45-12, pearlitic 100-70-03 and tempered martensitic (Q&T) 120-90-02.

The ductile cast iron results in the database generally exhibited the expected trends. Modulus and Poisson's ratio were the same for all the conditions. Monotonic strength always decreased with increasing elongation and ferrite content. The higher strength grades and conditions exhibited greater high cycle fatigue resistance and decreased low cycle fatigue resistance.

Heat treatments had a mixed effect on monotonic properties. Annealing decreased the monotonic strength of 60-40-18 whereas normalizing increased the strength and dramatically increased fatigue resistance of pearlitic 100-70-03. Monotonic ductility was only slightly affected by heat treatment.

However, in most conditions, the heat treatments produced greater low cycle fatigue lives for high ductility conditions. Although the high cycle fatigue resistance was affected less by heat treatment, slightly increased high cycle fatigue lives were obtained with higher strength conditions. The normalized 25 mm samples of grade 100-70-03 exhibited significantly greater monotonic strength as well as fatigue resistance in both the low and high cycle regime.

Keywords: *strain-life fatigue, low cycle fatigue, cast iron, ductile cast iron, microstructure, heat treatment*

Introduction

Description of Fatigue

A standard definition[1] of fatigue is that it is the process of progressive, localized, and permanent structural change occurring in a material subjected to conditions

- that produce fluctuating stresses and strains at some point or points, and
- that may culminate in cracks or complete fracture after a sufficient number of fluctuations.

Another common definition[2] introduces the concepts that

- fatigue fractures occur at fluctuating stresses with a maximum value less than the ultimate tensile strength of the material,
- fatigue failure generally occurs at loads which applied statically would produce little perceptible effect, and
- fatigue fractures begin as minute cracks that grow under the action of fluctuating stress.

High versus Low Cycle Fatigue

For over hundred years, the stress-life or S-N method was the first approach used in an attempt to quantify and design by fatigue. Although the S-N approach can be used in design applications where the applied stress is primarily within the elastic range of material response, the strain-life approach is required for low cycle fatigue life predictions between 10 and 100,000 cycles.[3]

The low cycle or strain-life approach also offers the advantage that both fatigue stress and strain are tested, analyzed, and modeled. Although high cycle fatigue only handles stress, low cycle or strain-life fatigue testing offers the opportunity for stress and strain to be calculated from each other. It is nearly impossible to measure stress with load cells in complex and moving structures, whereas strain can be readily measured with optical or strain gauge methods.

Another key difference between high and low cycle fatigue is that high cycle fatigue is strength and crack-initiation controlled where stronger materials exhibit greater fatigue lives in the high cycle range. High cycle fatigue testing commonly produces an endurance or fatigue limit (strength) at long lives (10 million cycles). The fatigue limit for p %survival is defined as the limiting value of fatigue strength for p %survival as N becomes very large (like 10 million cycles), where p may be any number, such as 95, 90, and so forth.[1] Low cycle fatigue on the other hand considers the regime where ductility and crack propagation dominate life such that more ductile materials exhibit greater fatigue lives in the low cycle range.

For several reasons, bending fatigue strength has been a property that was measured historically. Now, modern designers require low cycle or strain-life fatigue properties of cast iron to populate their computer-aided design databases so that cast iron can be compared to compendia[4] of strain-life properties of steels and other competing materials. Strain-life fatigue properties can not be determined in bending and must be determined axially so that the cyclic stress and strain can be related.

Another important distinction is that modern fatigue databases do not contain fatigue limits, which are essentially the stresses below which materials are expected to survive fatigue. Rather, finite element modeling programs must be able to predict lives and locations of fatigue fractures in the vicinity of holes, thickness changes, and other stress concentrators. The cast iron strain-life fatigue database discussed in this paper offers designers the opportunity to perform such calculations with cast iron.

Motivation for the Database

Strain-life fatigue testing was conducted on a variety of cast irons for a variety of reasons. Such fatigue data is intended for use in current endurance modeling methods. Thus, designers can select optimal materials and design geometries to foster

(a) lighter products,
(b) energy efficient operations,
(c) longer and more predictable product service life, and
(d) more energy efficient product manufacture.

Database Description

Multiple grades of a variety of cast irons were subjected to a considerable variety of tests, and a database containing the strain-life fatigue properties of multiple grades of cast iron was developed and published[5] in 2003. The work was originally funded by the U.S. Department of Energy/Cast Metals Coalition (DOE/CMC)[6] with guidance by the American Foundry Society (AFS). Since the publication of the original DOE report,[7] additional grades have been tested and the database contents have been augmented on an ongoing basis with additional AFS research funds. AFS has also developed an on-line materials database searching tool called CADS, which will eventually include this strain-life fatigue database product. For information see: http://www.metalcastingvirtuallibrary.com/cads/cads.aspx

Table 1 shows the current contents of the database based on testing by the author.[5] The database also contains contributed datasets from other sources, but these results are not included in the analysis conducted for this paper. Test samples for most of the grades were obtained from Y-blocks in the as-cast condition, but a few grades were tested with heat treated Y-blocks or with specimens machined from cast parts.

Table 1. Materials Tested at Element (as of March 2012)
The conditions marked in yellow were selected for analysis in this paper.

Austempered Ductile Iron: ASTM A 897-06		
ASTM Grade	*Material Condition*	*Section Size*
110 / 70 / 11	Austempered	48 mm by 43 mm by 185 mm section of rectangular casting
125 – 80 – 10 (130 / 90 / 09)		25 mm Y-block
150 – 100 – 7 (150 / 110 / 07)		
175 – 125 – 4		
200 – 155 – 1		
Ductile Iron: ASTM A 536-84 (Re 1999)		
ASTM Grade	*Material Condition*	*Section Size*
60 – 40 – 18	As-cast	25 mm Keel block
	Subcritical Anneal	25 mm Keel block
	Full Anneal	25 mm Y-block
	Heavy Section; As-Cast	76 mm Y-block
65 – 45 - 12	As-cast	25 mm Keel block
100 – 70 – 03	As-cast	25 mm Keel block
	Normalized	25 mm Keel block
		76 mm Y-block
120 – 90 – 02	Quenched and Tempered	25 mm Keel block
Compacted Graphite Iron: ASTM A 842-85(Re 1997)		
ASTM Grade	*Material Condition*	*Section Size*
300	As-Cast	25 mm Y-block
350		
400	As-Cast	25 mm Y-block
	As-Cast	**76 mm Y-block**
Gray Iron: ASTM A 48-00		
ASTM Grade	*Material Condition*	*Section Size*
20B	As-Cast	25 mm Y-block
30B	As-Cast	13 mm Round
	As-Cast	25 mm Y-block
	As-Cast	76 mm Y-block
35B	As-Cast	25 mm Y-block
40B	As-Cast with C.E.= 3.7	25 mm Y-block
	As-Cast with Normal C.E. = 4.0	25 mm Y-block
Austempered Gray Iron: No Standard Specification		
Base Iron	*Material Condition*	*Section Size*
Class 30B	Austempered	25 mm Y-block
Abrasion-Resistant Cast Iron: ASTM A 532		
ASTM Grade	*Material Condition*	*Section Size*
Class III Type A Level 2 (25%Cr)	Quenched & tempered	16 mm rectangular bars

Experimental Procedures

This section of this paper is highly abbreviated versus the original publication[5] describing the database. The original database project utilized differing procedures for different types of cast iron. This paper only addresses ductile iron, so only the procedures used for ductile iron are contained herein. Furthermore, operative ASTM test methods are only contained in the original publication.

Chemical Analysis and Metallography

An analysis of alloy chemistry was conducted on each of two samples extracted from randomly selected castings from each group of test materials. The concentrations of most elements were determined using optical emission spectrometry (OES) except carbon, nitrogen, and sulfur, which were determined using combustometric methods. Copper and magnesium were determined by atomic absorption (AA) spectrophotometry.

Typically, three metallographic specimens were prepared and analyzed for each test material. Transverse cross-sections were extracted from the gage section of tensile bars, mounted and polished using standard metallographic techniques. The samples were final polished using colloidal silica media with a 0.05 um particle size. The samples were photographed at two or three appropriate magnifications in the as-polished condition and after etching with 2% Nital. Automated image analysis was performed to measure nodularity, nodule count, and ferrite/pearlite content.

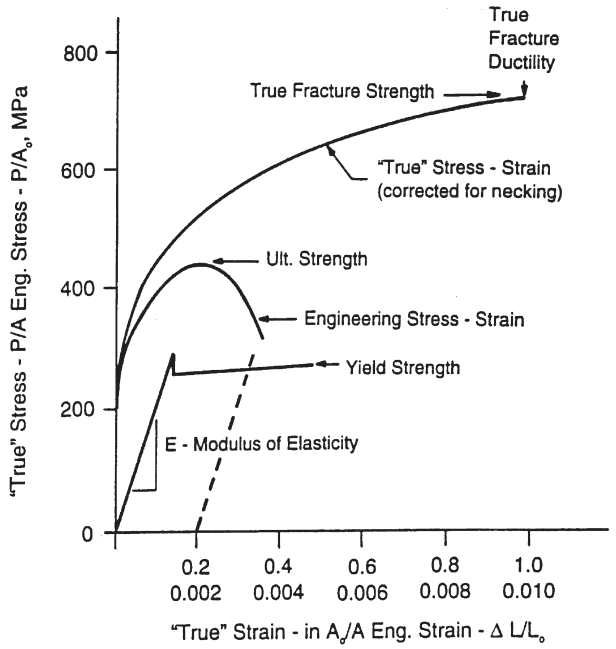

Figure 1. Engineering and true stress-strain plots and properties from Reference 4.

Hardness and Tensile Testing

Brinell hardness measurements were conducted on the shoulders of fractured tensile bars using a 3000 kg load. Tensile specimens were tested to determine standard tensile properties [i.e., 0.2% offset yield strength (S_y or YS), ultimate tensile strength (S_u or UTS), total elongation (%El), and reduction in area (%RA)]. Additionally, the monotonic tensile stress-strain response was characterized for a subset of the specimens in terms of elastic modulus and/or Poisson's ratio as well as monotonic strength coefficient (K) and monotonic strain hardening exponent (n). Figures 1 and 2 show the standard tensile properties and monotonic stress-strain constants, respectively.[4]

Room temperature tensile tests were conducted on standard round tensile specimens with 0.5 inch (13 mm) gauge diameter and 2.0 inch (50 mm) gauge length. In isolated cases, proportional subsize tension specimens were used when necessitated by material size constraints.

Strain gauges were employed for precision modulus and Poisson's ratio determinations and an extensometer was employed for determining K and n. For standard tension tests, an initial strain-rate of 0.3% per minute was imposed until the yield strength was exceeded; after yield, the strain-rate was increased to 10% per minute. The total elongation was measured by reassembly of the samples and physical measurement of the final gauge length. For elastic modulus or Poisson's ratio determination, a smaller initial strain rate of 0.2% per minute was used.

Fatigue Testing

All fatigue test specimens were machined with low stress procedures and longitudinally polished. The specimens had a 0.314 inch (8 mm) gage diameter, 0.628 inch (16 mm) gage length, 2.51 inch (64 mm) blending radius, and 0.590 inch (15 mm) diameter grip ends.

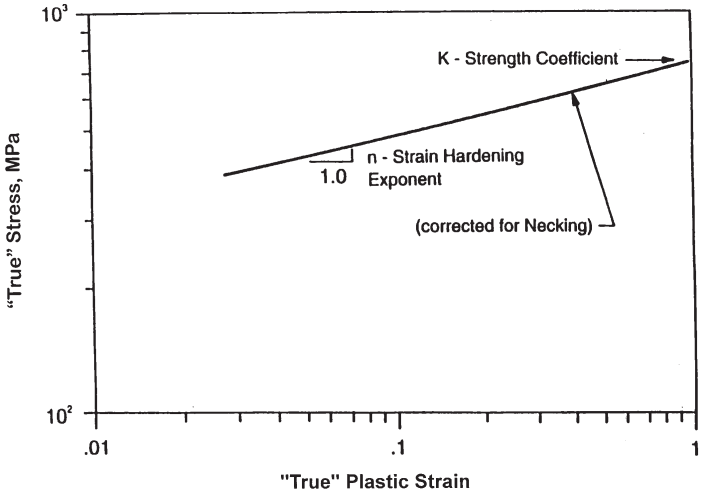

Figure 2. Logarithmic true stress-plastic strain plot with monotonic stress-strain constants from Reference 4.

Strain-controlled fatigue tests were conducted at room temperature over the range from about 100 cycles to 1,000,000 cycles. Generally, three specimens were tested at each of six to seven strain levels, and all tests were performed using a triangular waveform at a constant strain rate of 2% per second.

Specimens with anticipated fatigue lives in excess of 500,000 cycles were switched to stress-controlled testing after 100,000 cycles and thereafter were tested at a constant frequency of 15 cycles/second. Tests were continued until a 20% drop in stress range (~ 50% load drop in cast iron) occurred, or until 5,000,000 cycles were reached without failure. Strain and load data were recorded during the tests.

Fatigue Data Analysis

This section of the paper summarizes the strain-life fatigue data analysis that was conducted in the database development effort.[7] The reader is directed to other references for further details.[3,4,7,8]

A fundamental step in the strain-life analysis of cyclic property data is the decomposition of the total cyclic strain amplitude ($\Delta\varepsilon_t/2$) or ($\Delta\varepsilon/2$) into its component strains, i.e., plastic strain amplitude ($\Delta\varepsilon_p/2$) and elastic strain amplitude ($\Delta\varepsilon_e/2$) according to the equation:

$$(\Delta\varepsilon/2) = (\Delta\varepsilon_e/2) + (\Delta\varepsilon_p/2) \qquad \text{Eqn. 1}$$

In practice, the elastic component of strain is determined by dividing the stress amplitude ($\Delta\sigma/2$) at specimen half-life ($0.5N_f$) by the elastic modulus (E). The plastic strain amplitude is then given as the difference between the total strain amplitude and the elastic strain amplitude. Figure 3 shows the definition of the stress and strain ranges, which are twice their amplitude counterparts. The plastic strain data determined by this method are used in the calculation of both the strain/stress-life and cyclic stress-strain constants.

Using data obtained from each fatigue specimen at half-life, the cyclic stress-strain constants n' (cyclic strain hardening exponent) and K' (cyclic strength coefficient) were determined by regressing the stress amplitude ($\Delta\sigma/2$) versus plastic strain amplitude ($\Delta\varepsilon_p/2$) in logarithmic coordinates. Figure 4 shows the cyclic stress-strain constants, which are related as follows:

$$\Delta\sigma/2 = K'(\Delta\varepsilon_p/2)^{n'} \qquad \text{Eqn. 2}$$

The cyclic stress-strain constants K' and n' were also calculated directly from the strain-life constants.

The cyclic stress-life and strain-life constants σ'_f, b, ε'_f, and c were calculated as follows:

$$\Delta\sigma/2 = \sigma'_f(2N_f)^b \qquad \text{Eqn. 3}$$

Where:

$\Delta\sigma/2$ = true stress amplitude
$2N_f$ = reversals to failure (1 reversal = ½ cycle)
σ'_f = fatigue strength coefficient
b = fatigue strength exponent

as shown in Figure 5; and

$$\Delta\varepsilon_p/2 = \varepsilon'_f(2N_f)^c \qquad \text{Eqn. 4}$$

Where:

$\Delta\varepsilon_p/2$ = plastic strain amplitude
$2N_f$ = reversals to failure
ε'_f = fatigue ductility coefficient
c = fatigue ductility exponent

as shown in Figure 6.

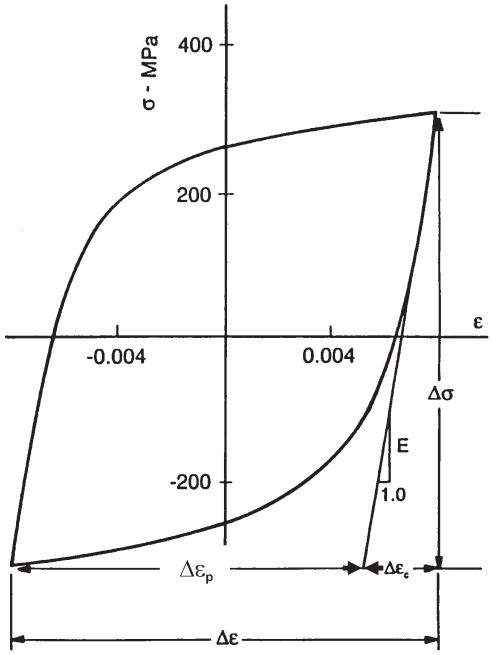

Figure 3. Stable hysteresis loop at half-life, showing the definitions of stress, total strain, elastic strain, and plastic strain ranges from Reference 4.

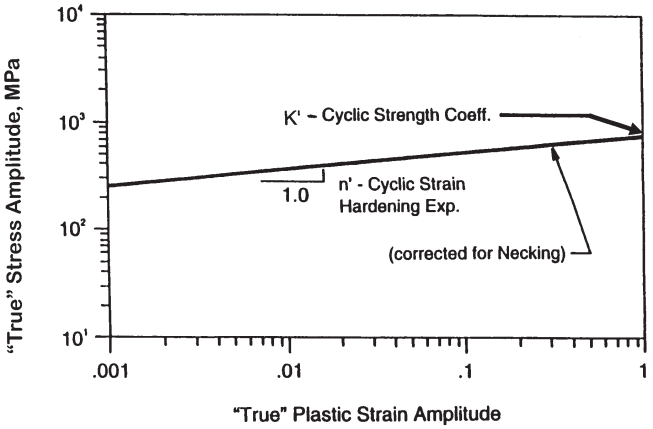

Figure 4. Logarithmic cyclic stress-plastic strain plot with cyclic stress-strain constants from Reference 4.

As discussed previously, the total strain is the sum of the elastic and plastic strains. In terms of strain amplitude,

$$\Delta\varepsilon/2 = \Delta\varepsilon_e/2 + \Delta\varepsilon_p/2 \qquad \text{Eqn. 5}$$

The elastic term can be written as:

$$\Delta\varepsilon_e/2 = \Delta\sigma/2E \qquad \text{Eqn. 6}$$

We can now state this in terms of reversals to failure:

$$\Delta\varepsilon_e/2 = (\sigma'_f / E) \times (2N_f)^b \qquad \text{Eqn. 7}$$

The plastic term is:

$$\Delta\varepsilon_p/2 = \varepsilon'_f (2N_f)^c \qquad \text{Eqn. 8}$$

The total strain can now be rewritten:

$$\Delta\varepsilon/2 = (\sigma'_f / E) \times (2N_f)^b + \varepsilon'_f (2N_f)^c \qquad \text{Eqn. 9}$$

This last equation is the basis of the strain-life method and is termed the strain-life relation, as shown in Figure 7.

It is sometimes useful to calculate the transition fatigue life (N_t), which is one definition for the fatigue life that is the boundary between low and high cycle fatigue. By replacing N_t for N_f in the above equations for elastic strain amplitude and plastic strain amplitude, the following equation is obtained:

$$N_t = \tfrac{1}{2} (\varepsilon'_f E / \sigma'_f)^{1/(b-c)} \qquad \text{Eqn. 10}$$

The cyclic stress-strain constants K' and n' were also calculated directly from the strain-life and stress-life constants as follows:

$$K' = \sigma'_f/(\varepsilon'_f)^{n'}$$
$$n' = b/c$$

Thus, the database contains K' and n' constants that were calculated by two methods, i.e., direct log-linear regression of the stress and plastic strain amplitudes and simple manipulation with the above two equations. Only the K' and n' data obtained from the regression analyses will be discussed in this paper.

Results and Discussion

Database Contents

The database has a directory structure that is summarized in the report, and other computer files. A typical database page for the composition and microstructure austempered ductile iron is shown in Figure 8. A typical database page with monotonic properties, strain-life fatigue constants and curves is shown in Figure 9. These database pages show average values, but the raw fatigue data and micrographs are also contained in the database. The turquoise-shaded regions are contributed datasets.

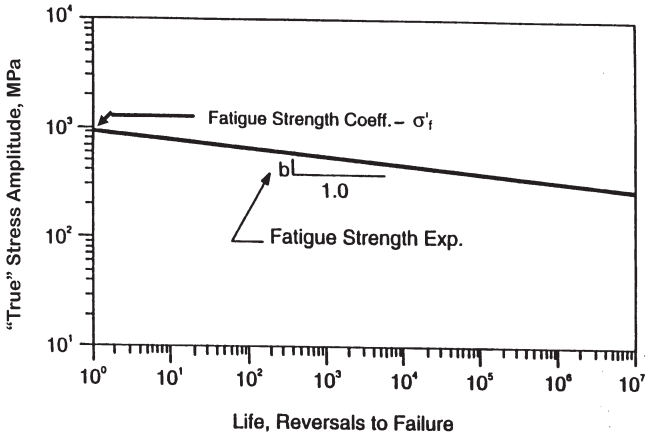

Figure 5. Logarithmic stress amplitude versus reversals plot from Reference 4.

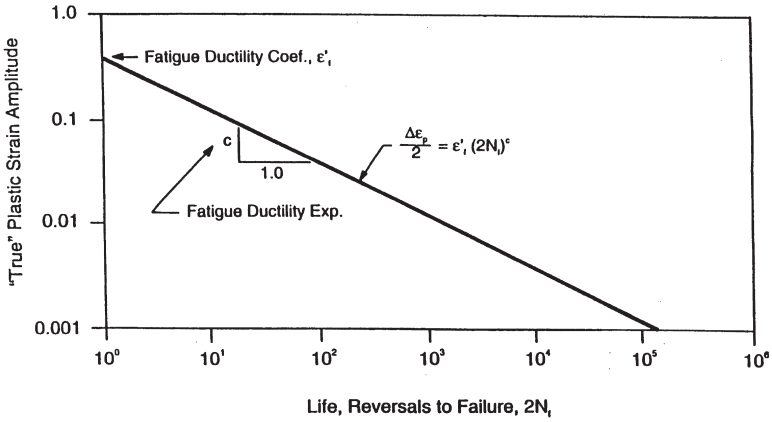

Figure 6. Logarithmic plastic strain amplitude versus reversals plot from Reference 4.

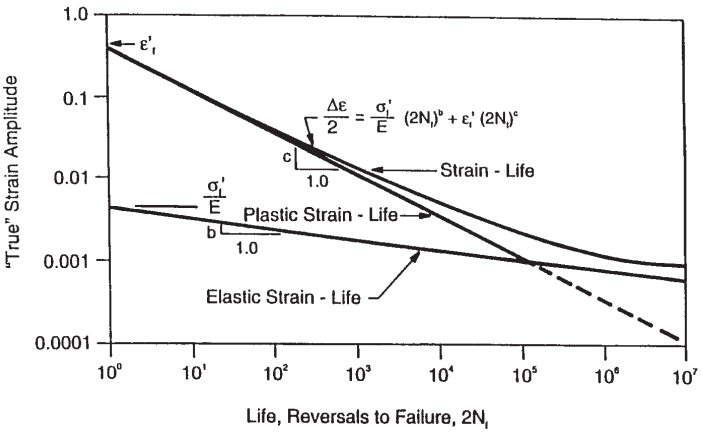

Figure 7. Logarithmic total strain amplitude versus reversals plot from Reference 4, showing the addition of the logarithmic elastic strain and plastic strain versus reversals lines.

Iron Type		Austempered Ductile Iron											
Grade: ASTM A 897/A 897M		125-80-10 [850-550-10]			150-100-7 [1050-700-7]			175-125-04 [1200-850-04]			200-155-01 [1400-1100-01]		
Material Condition		ASTM Standard	Austempered	Austempered	ASTM Standard	Austempered	Austempered	ASTM Standard	Austempered	Austempered	ASTM Standard	Austempered	Austempered
Cast Section Size			25 mm Y-block	~25 mm section		25 mm Y-block	~25 mm section		25 mm Y-block	~25 mm section		25 mm Y-block	~25 mm section
Material Code (Folder Title)			Grd 1 25mm	Grd 1 (lit)		Grd 2 25mm	Grd 2 (contrb)		Grd 3 25mm	Grd 3 (contrb)		Grd 4 25mm	Grd 4 (contrb)
Microstructure													
Nodularity (%)		-	94	-	-	94	-	-	94	-	-	94	-
Nodule Count (mm^{-2})		-	112	-	-	112	-	-	112	-	-	112	-
Nodule Size Distribution (%) (ASTM A-247)	7	-	19	-	-	19	-	-	19	-	-	19	-
	6	-	48	-	-	48	-	-	48	-	-	48	-
	5	-	33	-	-	33	-	-	33	-	-	33	-
	4	-	1	-	-	1	-	-	1	-	-	1	-
Matrix Composition		*Substantially Austenite & Acicular Ferrite*	Austenite & Acicular Ferrite	Austenite & Acicular Ferrite	*Substantially Austenite & Acicular Ferrite*	Austenite & Acicular Ferrite	Austenite & Acicular Ferrite	*Substantially Austenite & Acicular Ferrite*	Austenite & Acicular Ferrite	Austenite & Acicular Ferrite	*Substantially Austenite & Acicular Ferrite*	Austenite & Acicular Ferrite	Austenite & Acicular Ferrite
Chemical Analysis													
Element (wt%)	C	-	3.61	-	-	3.61	-	-	3.61	-	-	3.61	-
	C.E. = %C + 1/3(%Si)	-	4.45	-	-	4.45	-	-	4.45	-	-	4.45	-
	S	-	0.016	-	-	0.016	-	-	0.016	-	-	0.016	-
	P	-	0.012	-	-	0.012	-	-	0.012	-	-	0.012	-
	Si	-	2.52	-	-	2.52	-	-	2.52	-	-	2.52	-
	Mn	-	0.27	-	-	0.27	-	-	0.27	-	-	0.27	-
	Cr	-	0.03	-	-	0.03	-	-	0.03	-	-	0.03	-
	Ni	-	0.29	-	-	0.29	-	-	0.29	-	-	0.29	-
	Mo	-	<0.01	-	-	<0.01	-	-	<0.01	-	-	<0.01	-
	Al	-	0.12	-	-	0.12	-	-	0.12	-	-	0.12	-
	Cu	-	0.54	-	-	0.54	-	-	0.54	-	-	0.54	-
	Mg	-	0.056	-	-	0.056	-	-	0.056	-	-	0.056	-
	Ti	-	0.01	-	-	0.01	-	-	0.01	-	-	0.01	-
	Ce	-	0.0056	-	-	0.0056	-	-	0.0056	-	-	0.0056	-
	Sn	-	0.005	-	-	0.005	-	-	0.005	-	-	0.005	-

Figure 8. Typical database page with composition and quantitative microstructural results. This figure shows results for four tested grades and the contributed dataset shaded in turquoise and the literature dataset shaded in gray.

Iron Type	Austempered Ductile Iron											
Grade: ASTM A 897/A 897M	125-80-10 [850-550-10]			150-100-7 [1050-700-7]			175-125-04 [1200-850-04]			200-155-01 [1400-1100-01]		
Material Condition		Austempered	Austempered		Austempered	Austempered		Austempered	Austempered		Austempered	Austempered
Cast Section Size	*ASTM Standard*	25 mm Y-block	~25 mm section	*ASTM Standard*	25 mm Y-block	~25 mm section	*ASTM Standard*	25 mm Y-block	~25 mm section	*ASTM Standard*	25 mm Y-block	~25 mm section
Material Code (Folder Title)		Grd 1 25mm	Grd 1 (lit)		Grd 2 25mm	Grd 2 (contrb)		Grd 3 25mm	Grd 3 (contrb)		Grd 4 25mm	Grd 4 (contrb)
Monotonic Properties (Hardness and Tension)												
Brinell Hardness (HBW3000)	*269 - 321*[1]	304	302	*302 - 363*[1]	341	340	*341 - 444*[1]	390	387	*388 - 477*[1]	441	418
Ultimate Tensile Strength (S_U), ksi (MPa)	*>125 ksi*	153 (1060)	140 (966)	*> 150 ksi*	168 (1160)	165 (1140)	*> 175 ksi*	197 (1360)	190 (1310)	*> 200 ksi*	225 (1550)	220 (1520)
Tensile 0.2% Offset Yield Strength (S_{ys}), ksi (MPa)	*> 80 ksi*	109 (752)	110 (759)	*> 100 ksi*	126 (869)	130 (897)	*> 125 ksi*	157 (1080)	160 (1100)	*> 155 ksi*	180 (1240)	180 (1240)
Percent Elongation (%)	*> 10 %*	13.3	11	*> 7.0 %*	13	10	*> 4.0 %*	6.7	7	*> 1.0 %*	3.1	5
Percent Reduction in Area (%)	-	12	10	-	13	9	-	8.6	6	-	2.9	4
Strain Hardening Exponent (n)	-	0.16	0.143	-	0.124	-	-	0.085	-	-	0.148	-
Strength Coefficient (K), ksi (MPa)	-	231 (1600)	218 (1500)	-	238 (1640)	-	-	265 (1830)	-	-	386 (2660)	-
Elastic Modulus (E), ksi (MPa)	-	23800 (164000)	23600 (163000)	-	23600 (163000)	23200 (160000)	-	23100 (159000)	22900 (158000)	-	23300 (161000)	22600 (156000)
Poisson's Ratio (μ)	-	0.275	0.25	-	0.262	0.25	-	0.278	0.25	-	0.27	0.25
Cyclic Stress-Strain Properties												
Cyclic Strain Hardening Exponent (n')	-	0.125	0.1252	-	0.132	0.1376	-	0.116	0.1465	-	0.130	0.1600
Cyclic Strength Coefficient (K'), ksi (MPa)	-	235 (1620)	253 (1740)	-	279 (1920)	-	-	322 (2220)	-	-	467 (3120)	-
Strain-life Properties												
Fatigue Ductility Coefficient (ε'_f)	-	0.5255	0.1150	-	0.3452	0.1780	-	0.3951	0.3960	-	0.2323	0.4880
Fatigue Ductility Exponent (c)	-	-0.7391	-0.5940	-	-0.6970	-0.6280	-	-0.7855	-0.7520	-	-0.8224	-0.8480
Fatigue Strength Coefficient (σ'_f), ksi (MPa)	-	208.6 (1440)	211 (1460)	-	253.4 (1750)	394 (2720)	-	400.3 (2760)	450 (3100)	-	439 (3030)	728 (5020)
Fatigue Strength Exponent (b)	-	-0.0864	-0.0900	-	-0.0985	-0.1460	-	-0.1371	-0.1600	-	-0.1459	-0.2050

Footnotes

(1) These hardness ranges are only *typical* and are not ASTM requirements.

The gray shaded columns denote data taken from literature

The blue shaded columns denote contributed data. Although the strain-rates and waveforms used to generate the contributed data may differ from those used in tests conducted at CRS, the tests were reportedly conducted in accordance with ASTM

(a)

Figure 9. Typical database page with average monotonic properties and fatigue information. (a) This portion of the figure contains the average monotonic properties and fatigue constants for the four ADI grades tested for the database, and the two contributed datasets shaded in turquoise. (b) This portion of the figure shows the individual strain-life plots and regression results for one of the ADI grades.

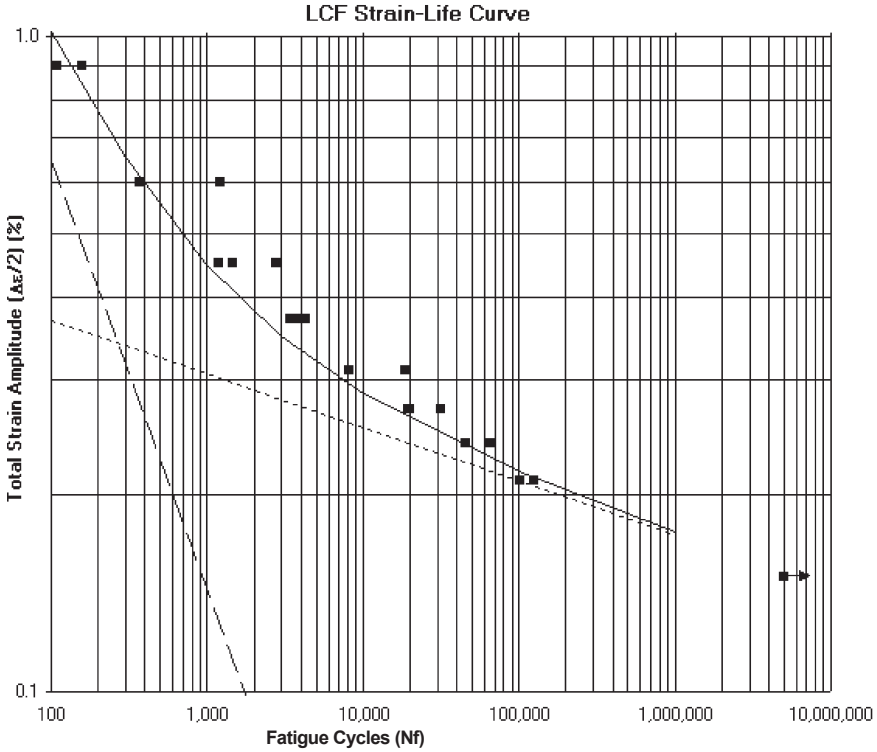

Customer: American Foundry Society (AFS)
Material: ADI750
Specimen Group: Round, 8 mm diameter
Waveform: Triangular
R-Ratio: -1
Test Temperature: Room Temperature
Test Machine: TestStar 10 kip

Project # 08-07-1485
Work Order # AME449-09-07-23394
Date: 8/31/09
Modulus: 25800 ksi
Yield Strength: 73 ksi
 # Samples Tested: 24
Control Parameter: Strain Rate, 2 %/s
Test Duration (Cycles): 5000000

Fatigue - Life Calculations

The fatigue life relationships listed in ASTM E606, Paragraph X1.1.2 were calculated using regression techniques to solve for fatigue life as a function of stress and strain.
The regression equations were then converted to the following standard forms:

$\Delta\sigma/2=\sigma' f * (2Nf)^b$

$\Delta\sigma/2 = 148 * (2Nf)^{-0.082}$ ksi $r^2 =$ 0.9530
$\Delta\sigma/2 = 1020 * (2Nf)^{-0.082}$ MPa

$\Delta\varepsilon\rho/2=\varepsilon' f * (2Nf)^c$

$\Delta\varepsilon\rho/2 = 0.2055 * (2Nf)^{-0.6527}$ $r^2 =$ 0.9600

$\Delta\varepsilon/2=(\sigma' f / E) * (2Nf)^b + \varepsilon' f * (2Nf)^c$

$\Delta\varepsilon/2 = 0.0057 * (2Nf)^{-0.082} + 0.2055 * (2Nf)^{-0.6527}$

Where the variables are:

$\Delta\sigma$ = true stress range
$\Delta\varepsilon\rho$ = true plastic strain range
$\Delta\varepsilon$ = true strain range
Nf = cycles to failure
2Nf = reversals to failure
r^2 = coefficients of determination

and the calculated constants are:

$\sigma' f$ = fatigue strength coefficient = 148 ksi
($\sigma' f$ = fatigue strength coefficient = 1020 MPa)
b = fatigue strength exponent = -0.082
$\varepsilon' f$ = fatigue ductility coefficient = 0.2055
c = fatigue ductility exponent = -0.6527
E = Young's modulus = 25.8 Mpsi
(E = Young's modulus = 178 GPa)
K' = cyclic strength coefficient = $\sigma' f / (\varepsilon' f)^{n'}$ = 180.5 ksi
(K' = cyclic strength coefficient = $\sigma' f / (\varepsilon' f)^{n'}$ = 1245 MPa)
n' = cyclic strain hardening exponent = b / c = 0.1256

(b)

Figure 9. Typical database page with average monotonic properties and fatigue information. (a) This portion of the figure contains the average monotonic properties and fatigue constants for the four ADI grades tested for the database, and the two contributed datasets shaded in turquoise. (b) This portion of the figure shows the individual strain-life plots and regression results for one of the ADI grades.

Data Selected for Analysis in this Paper

Some of the elemental contents and quantitative microstructural constituents are summarized in Table 2 for the eight selected conditions from Table 1. All subsequent figure numbers and legends in this paper are ordered with respect to the particular column that the condition occupies in Table 2.

The Table 2 results were chosen to display the most significant data for each of the selected conditions. Figures 10 to 17 each contain one example micrograph in the etched condition to illustrate each of the eight selected conditions.

Table 2. Abbreviated Elemental Contents and Microstructural Results for Selected Database Conditions

Grade: ASTM A 536 [SAE J434]		60-40-18 [D4018]			65-45-12 [D4512]	100-70-03 [D7003]			120-90-02
Material Condition		As-cast	Subcritical Anneal	Full Anneal	As-cast	As-cast	Normalized	Normalized	Quenched & Tempered
Cast Section Size		25 mm Keel-block	25 mm Keel-block	25 mm Y-block	25 mm Keel-block	25 mm Keel-block	25 mm Y-block	76 mm Y-block	25 mm Keel-block
Material Code (Folder Title)		4018-AC-25mm	4018-ScAn-25mm	4018-FAn-25mm	4512-AC-25mm	7003-AC-25mm	7003-N-25mm	7003-N-76mm	9002-QT-25mm
Microstructure									
Nodularity (%)		93	95	93	92	94	95	96	94
Nodule Count (mm^{-2})		264	246	202	112	271	153	40	299
Matrix Composition		81.3% Ferrite 18.7% Pearlite	Fully Ferritic	Fully Ferritic	54% Ferrite 46% Pearlite	8.7% Ferrite 91.3% Pearlite	8% Ferrite 92% Pearlite	1.7% Ferrite 98.3% Pearlite	Tempered Martensite
Chemical Analysis									
Element (wt%)	C	3.61	3.61	3.65	3.84	3.59	3.63	3.65	3.59
	C.E. = %C + 1/3(%SI)	4.50	4.50	4.53	4.61	4.35	4.50	4.52	4.35
	S	0.008	0.008	0.009	0.008	0.008	0.01	0.007	0.008
	P	0.026	0.026	0.016	0.02	0.02	0.023	0.026	0.02
	Si	2.66	2.66	2.63	2.31	2.29	2.6	2.6	2.29
	Mn	0.16	0.16	0.21	0.17	0.22	0.22	0.3	0.22
	Cu	0.25	0.25	0.15	0.32	0.85	0.23	0.6	0.85
	Mg	0.036	0.036	0.036	0.029	0.037	0.047	0.049	0.037
	Ce	0.0058	0.0058	0.0072	0.0038	0.0056	0.0035	0.0049	0.0056

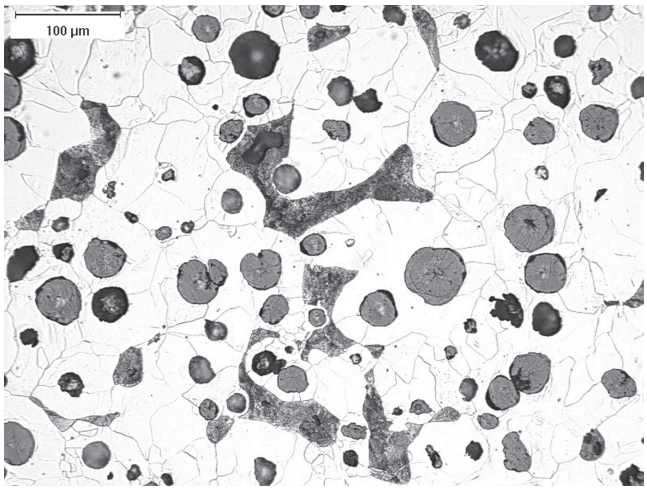

Figure 10. This optical micrograph corresponds to grade 60-40-18 in the as-cast condition. The original magnification is 200X.

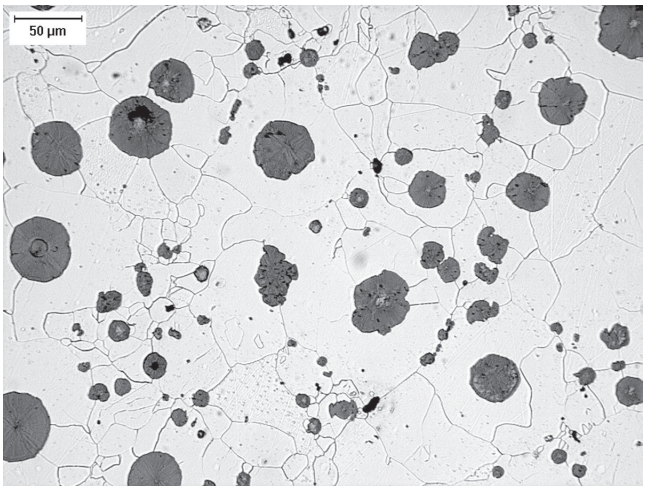

Figure 11. This optical micrograph corresponds to grade 60-40-18 in the subcritically annealed condition. The original magnification is 250X.

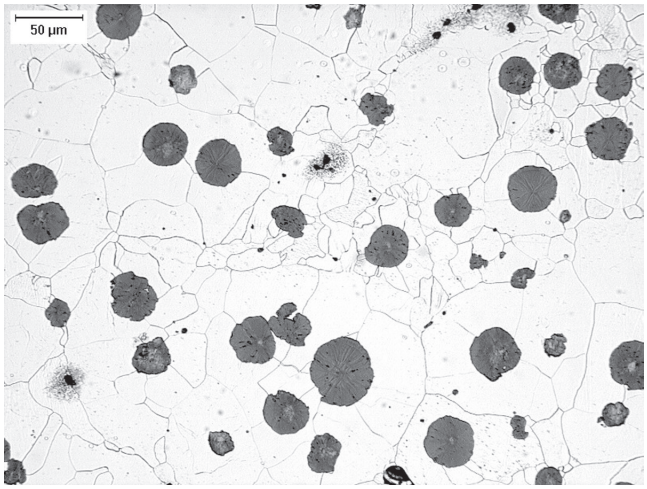

Figure 12. This optical micrograph corresponds to grade 60-40-18 in the fully annealed condition. The original magnification is 250X.

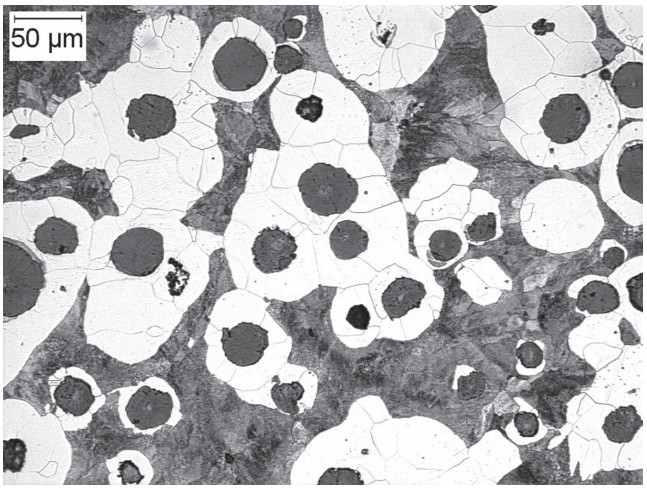

Figure 13. This optical micrograph corresponds to grade 65-45-12 in the as-cast condition. The original magnification is 250X.

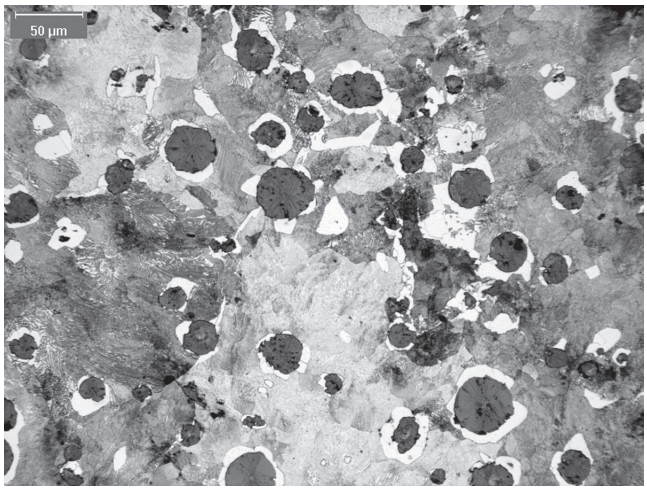

Figure 14. This optical micrograph corresponds to grade 100-70-13 in the as-cast condition. The original magnification is 250X.

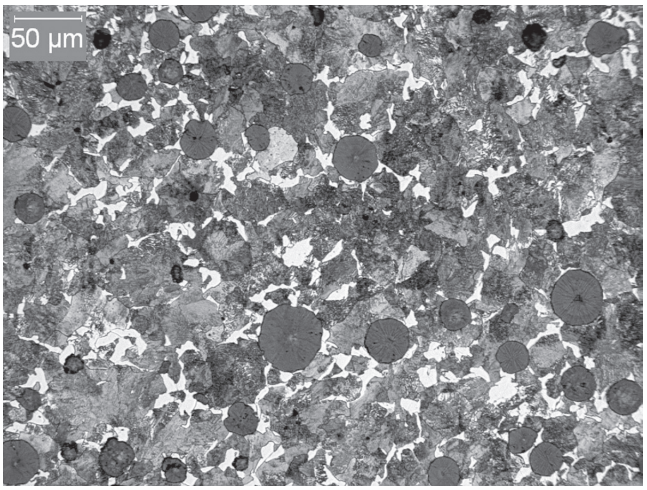

Figure 15. This optical micrograph corresponds to the 25 mm section size of grade 100-70-13 in the normalized condition. The original magnification is 250X.

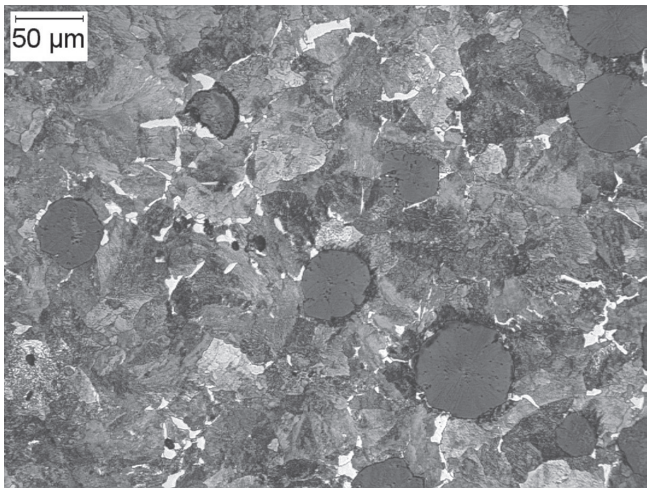

Figure 16. This optical micrograph corresponds to the 76 mm section size of grade 100-70-13 in the normalized condition. The original magnification is 250X.

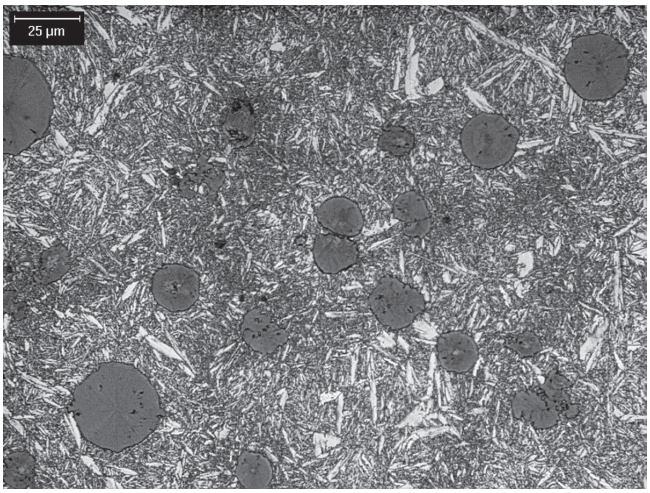

Figure 17. This optical micrograph corresponds to grade 120-90-02 in the quenched and tempered condition. The original magnification is 500X.

Compositions and Microstructures

Table 2 shows that all the as-cast and heat treated ductile cast irons have typical compositions for their corresponding ASTM[9] or SAE[10] grades, all have high nodularity (greater than 90%), and almost all have standard nodule counts between 100 to 300 mm^{-2}. Due to its heavier section size, the 76 mm section size for the 100-70-03 grade has lower nodule count than the other seven conditions.

The Table 2 results were chosen to display the most significant data for each of the selected conditions. Figures 10 to 17 each contain one example micrograph selected for each of the eight conditions.

The microstructures in the grades obeyed expectations as follows:

1. The ferrite content in the as-cast grades decreased with increasing strength and decreasing ductility in the first three grades listed in Table 2, as also shown in Figures 10, 13 and 14.
2. The ferrite contents in Table 2 and the micrographs in Figures 10 to 12 show that the annealing treatments converted the as-cast 60-40-18 grade to all ferrite, as expected.
3. For as-cast 100-70-03, Figure 14 shows that the ferrite surrounded nodules, and this is commonly called bulls-eye ferrite. After normalizing, Figures 15 and 16 show that the ferrite is more randomly distributed throughout the matrix.
4. For grade 120-90-02, Figure 17 shows that the ferrite-pearlite microstructure converted to tempered martensite after quenching and tempering (Q&T).

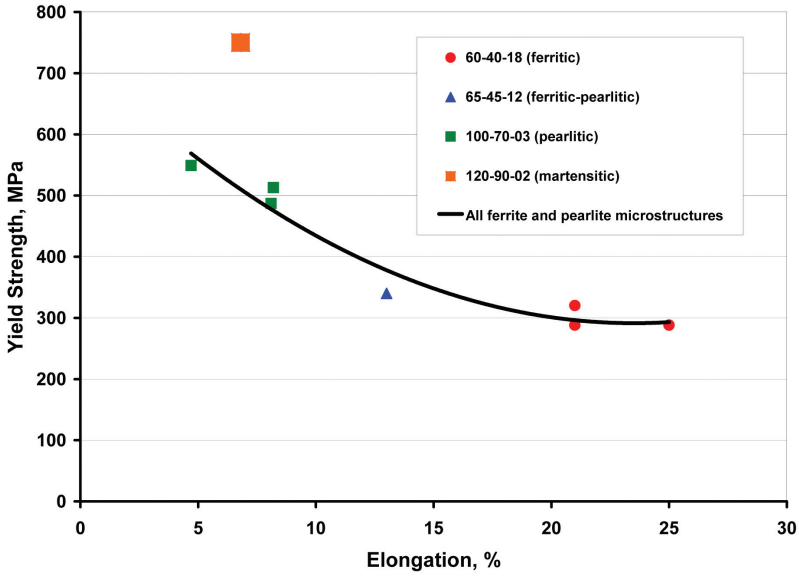

Figure 18. The yield strength and elongation of the ferrite and pearlite microstructures obeyed a quadratic relationship. The open points represent the heat treatment conditions and the closed points represent the as-cast condition. The tempered martensite microstructure had greater strength than the locus of points for the ferrite and pearlite grades.

Table 3. Monotonic Properties and Coefficients for Selected Database Conditions

Grade: ASTM A 536 [SAE J434]	**60-40-18 [D4018]**			**65-45-12 [D4512]**	**100-70-03 [D7003]**			**120-90-02**
Material Condition	As-cast	Subcritical Anneal	Full Anneal	As-cast	As-cast	Normalized	Normalized	Quenched & Tempered
Cast Section Size	25 mm Keel-block	25 mm Keel-block	25 mm Y-block	25 mm Keel-block	25 mm Keel-block	25 mm Y-block	76 mm Y-block	25 mm Keel-block
Material Code (Folder Title)	4018-AC-25mm	4018-ScAn-25mm	4018-FAn-25mm	4512-AC-25mm	7003-AC-25mm	7003-N-25mm	7003-N-76mm	9002-QT-25mm
Monotonic Properties (Hardness and Tension)								
Brinell Hardness (HBW3000)	161	154	150	186	259	269	285	296
Ultimate Tensile Strength (S_U), ksi (MPa)	69.6 (480)	66.5 (459)	64.2 (443)	84 (579)	121.3 (836)	128 (883)	129.5 (893)	133.7 (922)
0.2% Offset Yield Strength (S_{ys}), ksi (MPa)	46.9 (323)	46.4 (320)	41.7 (288)	49.3 (340)	70.6 (487)	74.4 (513)	79.6 (549)	108.8 (750)
Percent Elongation (%)	21	21	25	13	8.1	8.2	4.7	6.8
Percent Reduction in Area (%)	24	26	30	11	7.1	7.2	3.97	7.2
Strain Hardening Exponent (n)	0.175	0.16	0.18	0.216	-	0.252	0.279	0.119
Strength Coefficient (K), ksi (MPa)	114 (786)	107 (738)	103 (710)	154 (1060)	-	269 (1860)	324 (2230)	200 (1380)
Elastic Modulus (E), ksi (MPa)	25000 (172000)	25100 (173000)	24000 (165000)	25100 (173000)	24900 (172000)	24800 (171000)	25700 (177000)	24600 (170000)
Poisson's Ratio (μ)	0.289	0.287	0.282	0.288	-	0.287	0.293	0.278

Monotonic Mechanical Properties

Table 3 shows the monotonic mechanical properties that were obtained for the selected grades. Figure 18 shows a plot of yield strength versus elongation for all eight selected conditions. Selected mechanical properties are also plotted versus ferrite content in Figures 19 and 20 for the three as-cast conditions.

The monotonic mechanical properties in the as-cast condition obeyed expectations as follows:

1. Figure 18 shows that the yield strengths of the ferritic, ferritic-pearlitic, and pearlitic irons decreased with increasing elongation.
2. Figure 19 shows that the hardness, yield strength and tensile strength increased with decreasing ferrite content in the as-cast conditions.
3. Figure 19 shows that the ductility, as measured by both elongation and reduction in area, increased with increasing ferrite content in the as-cast conditions.

The monotonic mechanical properties were altered with heat treatment for the two grades that were evaluated, but less predictably. The following heat treatment trends were observed:

1. Table 3 shows that the tensile strength of as-cast grade 60-40-18 decreased slightly with subcritical annealing and decreased significantly with full annealing.
2. Table 3 shows that the yield strength of as-cast grade 60-40-18 decreased slightly with subcritical annealing and decreased significantly with full annealing.
3. Table 3 shows that the ductility of as-cast grade 60-40-18 hardly changed with subcritical annealing; however, significant increases in ductility were obtained with full annealing.
4. Table 3 shows that the yield and tensile strengths of the normalized 100-70-03 grade increased significantly with respect to the as-cast 100-70-03 grade in both the 25 mm and 76 mm section sizes. (In fact, the 100-70-03 properties are not generally obtainable in a heavy section size without normalizing.)
5. Table 3 shows that ductility of the 25 mm as-cast samples of the 100-70-03 grade did not change when they were normalized.
6. Table 3 shows that the ductility of the normalized 76 mm samples was significantly lower than the 25 mm samples of the 100-70-03.
7. Figure 18 shows that quenched and tempered (Q&T) grade 120-90-02 had a significantly higher yield strength at the same ductility of the pearlitic 100-70-03 grade.

No significant change in the elastic properties (modulus and Poisson's ratio) were observed for any of the conditions.

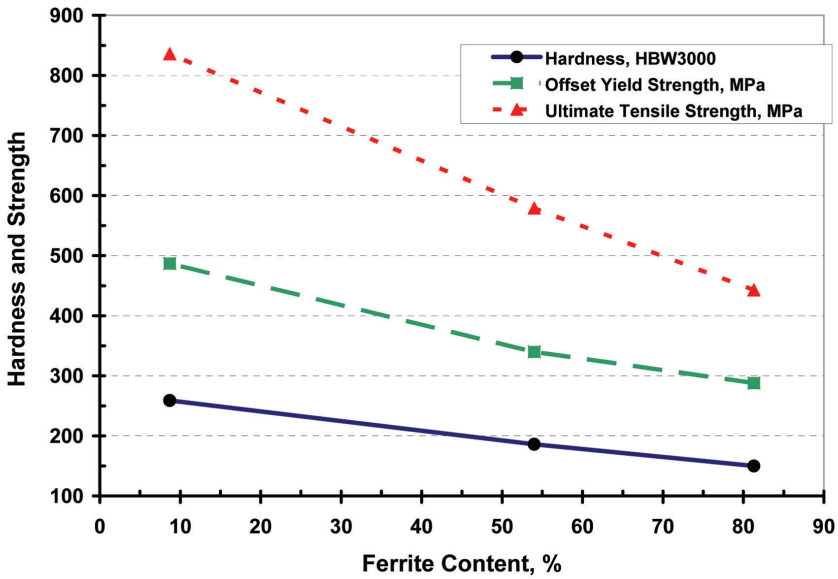

Figure 19. The hardness and strength decreased with increasing ferrite content for the as-cast conditions.

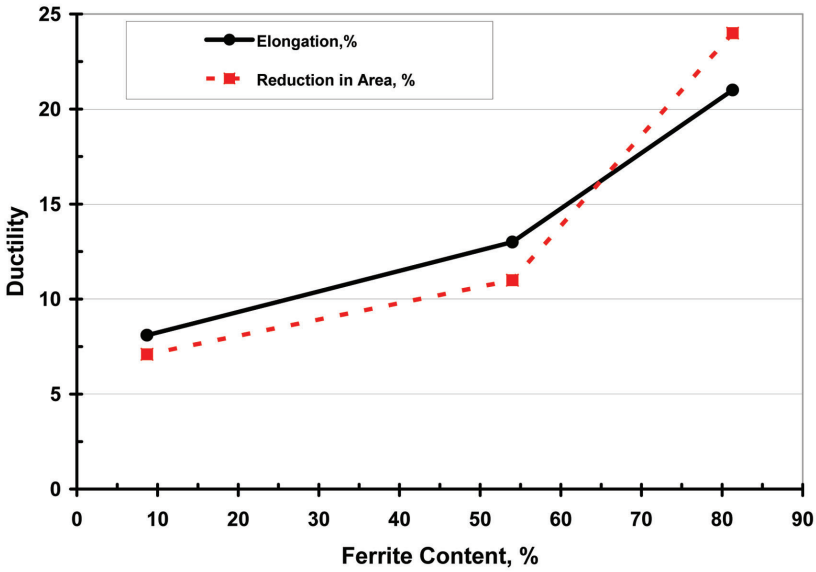

Figure 20. The ductility increased with increasing ferrite content for the as-cast conditions.

Strain-Life Fatigue Properties

Table 4 shows the cyclic fatigue constants that were obtained for the selected grades. Note that it is both difficult and not recommended to directly compare materials based on the constants alone. Similarities and differences among materials are best compared by strain-life plots, as discussed below.

Figure 21 shows a plot of the total strain versus fatigue cycles for four selected grades. In the plot legend, the grade is identified with the ASTM designation, but the actual UTS-YS-El values from Table 3 and ferrite contents from Table 2 are shown parenthetically. The plotted curves in Figure 21 are the total strain-life hyperbolas predicted from the results in Table 4. Actual fatigue data points are shown for three grades. Predicted fatigue lives are shown in Table 5.

The cyclic properties of the grades obeyed expectations as follows:

1. Figure 21 and Table 5 show that the higher strength grades had lower fatigue lives in the low cycle regime and higher fatigue lives in the high cycle regime.
2. Figure 21 and Table 5 show that the higher ductility grades had higher fatigue lives in the low cycle regime and lower fatigue lives in the high cycle regime.
3. These predicted trends were observable, but only showed significance for the extremes, i.e., the differences in fatigue lives were only significantly greater than the range of the data for the two extreme conditions (the 60-40-18 and 120-90-02 grades).

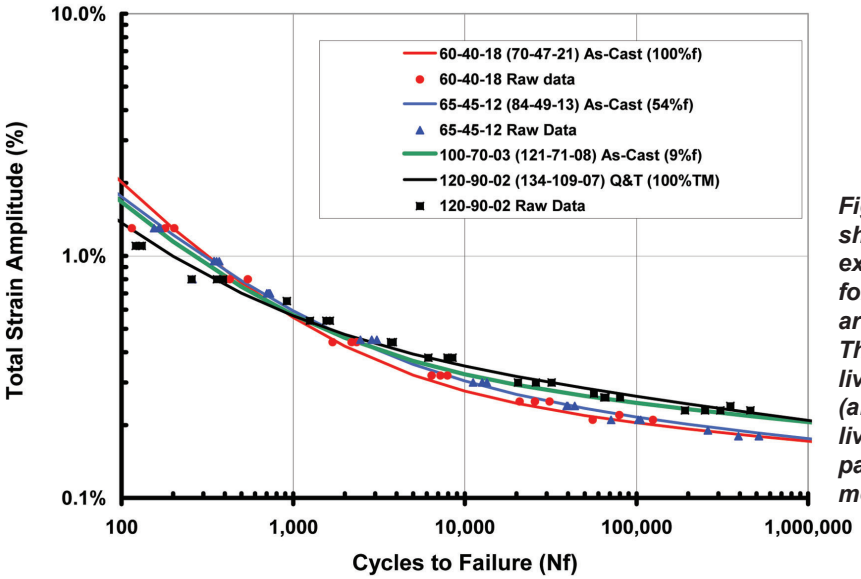

Figure 21. Total strain-life fatigue curves are shown as a function of grade and display the expected trends. The points are actual data for three selected grades and the curves are the predicted lives from constants. The higher strength grades exhibit greater lives at high cycles and the higher ductility (and lower strength) grades exhibit greater lives in the low cycle regime. The values in parentheses in the legend are the measured monotonic properties and ferrite contents.

Table 4. Low Cycle Fatigue Constants for Selected Database Conditions

Grade: ASTM A 536 [SAE J434]	60-40-18 [D4018]			65-45-12 [D4512]	100-70-03 [D7003]			120-90-02
Material Condition	As-cast	Subcritical Anneal	Full Anneal	As-cast	As-cast	Normalized	Normalized	Quenched & Tempered
Cast Section Size	25 mm Keel-block	25 mm Keel-block	25 mm Y-block	25 mm Keel-block	25 mm Keel-block	25 mm Y-block	76 mm Y-block	25 mm Keel-block
Material Code (Folder Title)	4018-AC-25mm	4018-ScAn-25mm	4018-FAn-25mm	4512-AC-25mm	7003-AC-25mm	7003-N-25mm	7003-N-76mm	9002-QT-25mm
Cyclic Stress-Strain Properties: Strain-life Method (ASTM E606; SAE J1099)								
Cyclic Strain Hardening Exponent (n')	0.073	0.074	0.053	0.094	0.087	0.105	0.122	0.091
Cyclic Strength Coefficient (K'), ksi (MPa)	98.8 (681)	97.8 (674)	85.2 (587)	115 (793)	137 (945)	156 (1080)	178 (1230)	172 (1190)
Strain-life Properties: Strain-life Method (ASTM E606; SAE J1099)								
Fatigue Ductility Coefficient (ε'_f)	0.5148	0.6016	0.9632	0.4482	0.5855	0.6648	0.2729	0.3694
Fatigue Ductility Exponent (c)	-0.6827	-0.7177	-0.7602	-0.6483	-0.7198	-0.6679	-0.6395	-0.7035
Fatigue Strength Coefficient (σ'_f), ksi (MPa)	102.1 (704)	103.3 (712)	99.5 (686)	109.9 (757)	134.2 (926)	163.8 (1130)	164.8 (1140)	191.7 (1320)
Fatigue Strength Exponent (b)	-0.0596	-0.0653	-0.0606	-0.0643	-0.0669	-0.0880	-0.0907	-0.0909
Transition Fatigue Life (N_t), cycles	1227	1041	1200	385	658	1420	461	274

Table 5 contains predictions and Figure 22 shows a plot of the total strain versus predicted fatigue cycles for the two heat treated ferritic-pearlitic grades (60-40-18 and 100-70-03), which had corresponding as-cast conditions. The cyclic properties of the heat treated grades generally obeyed expectations as follows:

1. In most conditions, the heat treatments produced greater low cycle fatigue lives for high ductility conditions
2. Although the high cycle fatigue resistance was affected less by heat treatment, slightly increased high cycle fatigue lives were obtained with higher strength conditions.
3. The normalized 25 mm samples of grade 100-70-03 exhibited significantly greater monotonic strength as well as fatigue resistance in both the low and high cycle regime.

Table 5 contains predictions and Figures 23 and 24 respectively show predicted stress-life and plastic strain-life fatigue curves as a function of grade. Table 4 shows no observable trends in transition fatigue life.

Summary and Conclusions

1. This paper reviewed the contents and architecture of the AFS strain-life fatigue database for cast iron.
2. As expected, the monotonic
   a. Yield strengths of the ferritic, ferritic-pearlitic, and pearlitic irons decreased with increasing elongation,
   b. Hardness, yield strength and tensile strength increased with decreasing ferrite content.
   c. Ductility increased with increasing ferrite content.
   d. Elastic modulus and Poisson's ratio were virtually identical for all the tested conditions.
3. The monotonic mechanical properties were altered with heat treatment for the 60-40-18 and 100-70-03 grades as follows:
   a. The yield and tensile strengths of as-cast grade 60-40-18 decreased slightly with subcritical annealing and decreased significantly with full annealing.
   b. The ductility of as-cast grade 60-40-18 hardly changed with subcritical annealing; however, significant increases in ductility were obtained with full annealing.

Table 5. Predicted Fatigue Lives from $\Delta\varepsilon_T/2 = (\sigma'_f/E)(2N_f)^b + (\varepsilon'_f)(2N_f)^c$ for Selected Database Conditions

Material & Alloy			60-40-18 (70-47-21) As-Cast (100%f)	60-40-18 (67-46-21) Subcritical Anneal (100%f)	60-40-18 (64-42-25) Full Anneal (81%f)	65-45-12 (84-49-13) As-Cast (54%f)	100-70-03 (121-71-08) As-Cast (9%f)	100-70-03 (128-74-08) Normalized (8%f)	100-70-03 (128-80-05) Normalized Heavy Section (2%f)	120-90-02 (134-109-07) Q&T (100%TM)
Condition Identifier		Cycles	4018-AC-25mm	4018-ScAn-25mm	4018-FAn-25mm	4512-AC-25mm	7003-AC-25mm	7003-N-25mm	7003-N-76mm	9002-QT-25mm
Stress Amplitude, MPa	$\Delta\sigma$ / 2	100	511	504	498	538	650	709	705	815
		1,000	444	433	433	464	557	579	572	661
		10,000	386	373	376	400	477	473	464	537
		100,000	336	321	327	345	409	386	377	435
		1,000,000	292	276	285	298	351	315	306	353
Elastic Strain Amplitude, %	$\Delta\varepsilon_e$ / 2	100	0.297%	0.291%	0.302%	0.311%	0.378%	0.415%	0.398%	0.480%
		1,000	0.258%	0.251%	0.262%	0.268%	0.324%	0.339%	0.323%	0.389%
		10,000	0.225%	0.216%	0.228%	0.231%	0.278%	0.276%	0.262%	0.316%
		100,000	0.195%	0.185%	0.198%	0.200%	0.238%	0.226%	0.213%	0.256%
		1,000,000	0.170%	0.160%	0.173%	0.172%	0.204%	0.184%	0.173%	0.208%
Plastic Strain Amplitude, %	$\Delta\varepsilon_p$ / 2	100	1.7158%	1.3423%	1.7158%	1.4445%	1.2919%	1.9312%	0.9215%	0.8886%
		1,000	0.2980%	0.2571%	0.2980%	0.3246%	0.2463%	0.4149%	0.2113%	0.1759%
		10,000	0.0518%	0.0493%	0.0518%	0.0730%	0.0470%	0.0891%	0.0485%	0.0348%
		100,000	0.0090%	0.0094%	0.0090%	0.0164%	0.0090%	0.0191%	0.0111%	0.0069%
		1,000,000	0.0016%	0.0018%	0.0016%	0.0037%	0.0017%	0.0041%	0.0025%	0.0014%
Total Strain Amplitude, %	$\Delta\varepsilon_T$ / 2	100	2.013%	1.634%	2.017%	1.756%	1.670%	2.346%	1.320%	1.368%
		1,000	0.556%	0.508%	0.560%	0.593%	0.570%	0.753%	0.535%	0.565%
		10,000	0.276%	0.265%	0.280%	0.304%	0.325%	0.366%	0.311%	0.350%
		100,000	0.204%	0.195%	0.207%	0.216%	0.247%	0.245%	0.224%	0.263%
		1,000,000	0.171%	0.161%	0.174%	0.176%	0.206%	0.188%	0.175%	0.209%

c. The yield and tensile strengths of the normalized 100-70-03 grade increased significantly with respect to the as-cast 100-70-03 grade in both the 25 mm and 76 mm section sizes.
d. The ductility of 25 mm as-cast samples of the 100-70-03 grade did not change when they were normalized.
e. The ductility of the normalized 76 mm samples was significantly lower than the 25 mm samples of the 100-70-03.
f. The quenched and tempered grade 120-90-02 had a significantly higher yield strength at the same ductility of the pearlitic 100-70-03 grade.

4. The cyclic properties of the grades obeyed expectations as follows:
   a. As compared to the lower strength grades, the higher strength grades had lower fatigue lives in the low cycle regime and higher fatigue lives in the high cycle regime.
   b. As compared to the lower ductility grades, the higher ductility grades had higher fatigue lives in the low cycle regime and lower fatigue lives in the high cycle regime.
   c. These predicted trends were observable, but only showed significance for the extremes, i.e., the differences in fatigue lives were only significantly greater than the range of the data for the two extreme conditions (the 60-40-18 and 120-90-02 grades).
5. No observable difference in transition (between the low and high cycle or plastic and elastic) fatigue life was observed.

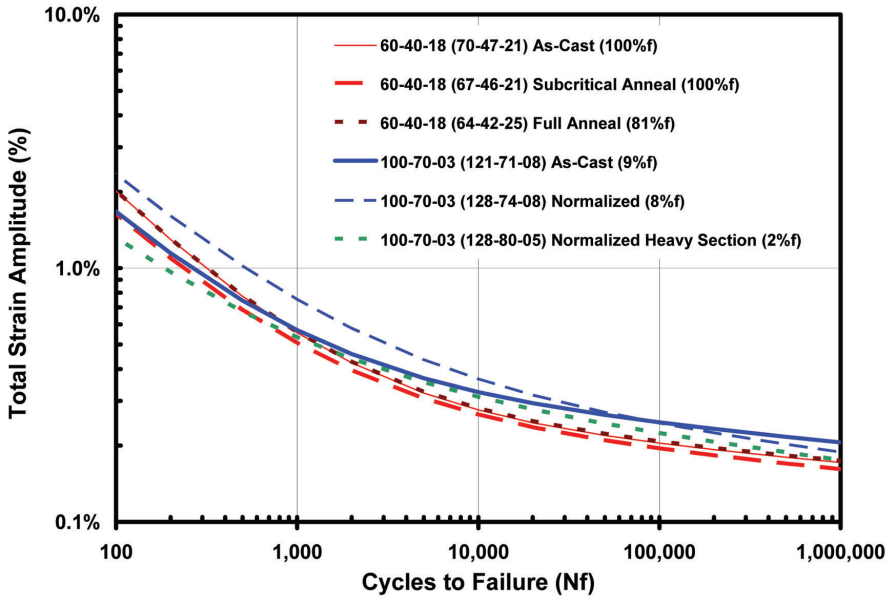

Figure 22. Total strain-life fatigue curves are shown for the two heat treated ferritic-pearlitic grades with corresponding as-cast conditions. The points are actual data for three selected grades and the curves are the predicted lives from constants. The values in parentheses in the legend are the measured monotonic properties and ferrite contents. In most conditions, the heat treatments did not significantly affect the predicted fatigue life for the as-cast condition, although similar strength and ductility trends to those shown in Figure 21 were observed. It is noteworthy that the normalized 25 mm samples of grade 100-70-03 exhibited significantly greater monotonic strength and fatigue resistance in both the low and high cycle regime.

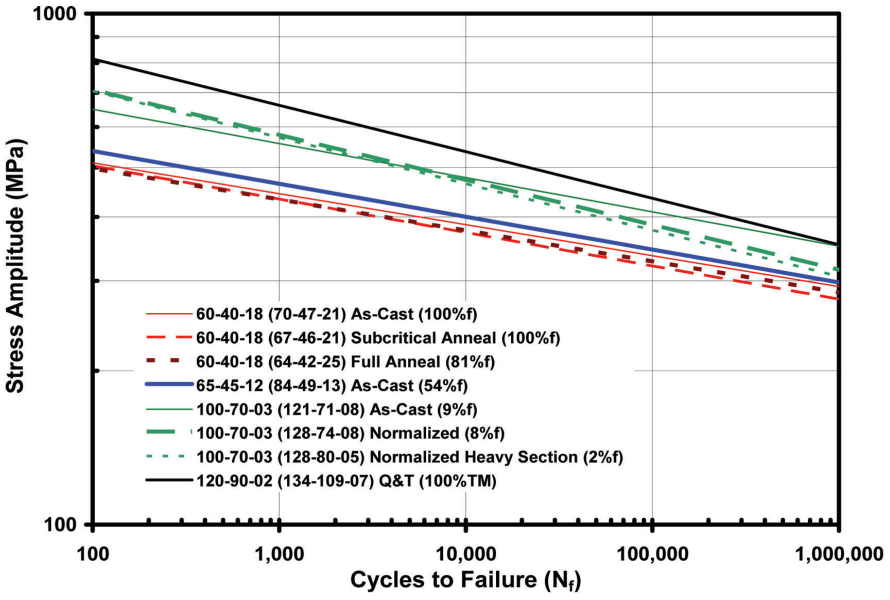

Figure 23. Predicted stress-life fatigue curves are shown as a function of grade and display the expected trends for all eight selected conditions. The higher strength grades exhibit greater lives at high cycles and decreased lives in the low cycle regime. The values in parentheses in the legend are the measured monotonic properties and ferrite contents.

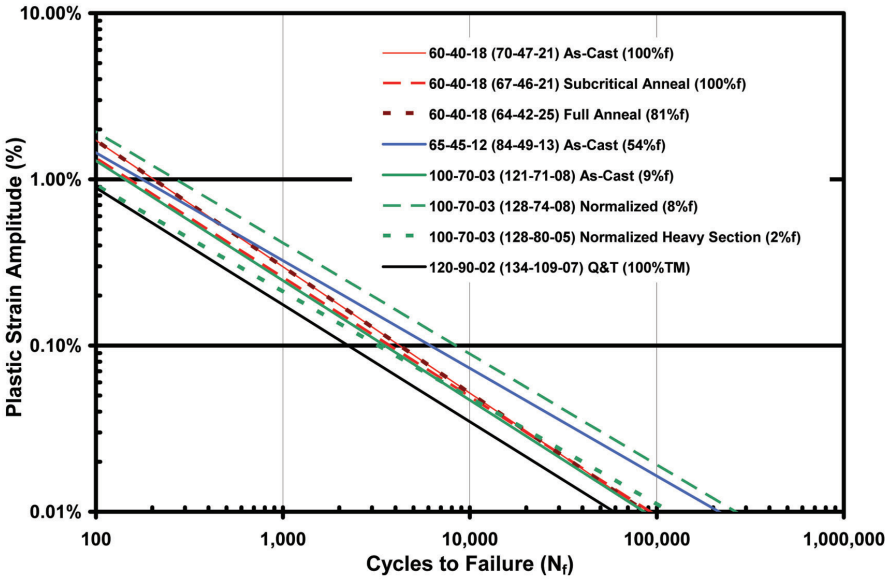

Figure 24. Predicted plastic strain-life fatigue curves are shown as a function of grade and display the expected trends for all eight selected conditions. The higher ductility grades exhibit greater lives at low cycles and decreased lives in the high cycle regime. The values in parentheses in the legend are the measured monotonic properties and ferrite contents.

Acknowledgments

The author gratefully acknowledges the research support from American Foundry Society (AFS) and helpful comments from Richard B. Gundlach of Stork CRS.

This research was sponsored under the AMC Casting for Improved Readiness (CIR) program by the Defense Supply Center, Philadelphia, PA and the Defense Logistics Agency, Ft. Belvoir, VA.

REFERENCES

1. ASTM Standard E 1823, 2010a, "Standard Terminology Relating to Fatigue and Fracture Testing," ASTM International, West Conshohocken, PA, 2010, DOI: 10.1520/E1823-10A, www.astm.org
2. Davis, J.R., Editor, "ASM Materials Engineering Dictionary," ASM International, Materials Park, OH, 1992.
3. Bannantine, J.A., Comer, J. S., Hancock, J. L. "Fundamentals of Metal Fatigue Analysis," Prentice-Hall, Inc., Upper Saddle River, NJ, 1990.
4. SAE Standard J1099, "Technical Report on Low Cycle Fatigue Properties Ferrous and Non-Ferrous Materials," SAE International, Warrendale, PA, August, 2002.
5. DeLa'O, James D., Gundlach, R. B. and Tartaglia, J. M., "Strain-Life Fatigue Properties Database for Cast Iron (DVD), ISBN: 978-0-87433-331-2, RR08DVD, www.afsinc.org
6. DOE/CMD Cooperative Agreement DE-FC07-00ID13852
7. "Development of a Cast Iron Fatigue Properties Database for Use in Modern Design Methods," Final Technical Report No. DOE/ID13852, DOE Contract No. DE-FC07-00ID13852, September 28, 2003.
8. ASTM Standard E606, 04e1, "Standard Practice for Strain-Controlled Fatigue Testing," ASTM International, West Conshohocken, PA, 2010, DOI: 10.1520/E0606-04E01, www.astm.org
9. ASTM Standard A536, 84 (2009), "Standard Specification for Ductile Iron Castings," ASTM International, West Conshohocken, PA, 2010, DOI: 10.1520/A0536-84R09, www.astm.org
10. SAE Standard J434, "Surface Vehicle Standard on Automotive Ductile (Nodular) Iron Castings," SAE International, Warrendale, PA, February, 2004.